68650 V2

Economics of Adaptation to Climate Change

Annexes

ETHIOPIA

Economics of Adaptation to Climate Change

ETHIOPIA

THE WORLD BANK

Ministry of Foreign Affairs
Government of the Netherlands

DFID Department for International Development
UNITED KINGDOM

Schweizerische Eidgenossenschaft
Confédération suisse
Confederazione Svizzera
Confederaziun svizra

Swiss Agency for Development
and Cooperation SDC

1818 H Street, NW
Washington, DC 20433
Telephone: 202-473-1000
Internet: www.worldbank.org
E-mail: feedback@worldbank.org

Annex 1

CLIRUN- II Rainfall Runoff Model Description

BACKGROUND

CLIRUN-II is the latest model in a family of hydrologic models developed specifically for the analysis of the impact of climate change on runoff. Kaczmarek (1993) presents the theoretical development for a single-layer lumped watershed rainfall runoff model-CLIRUN. Kaczmarek (1998) presents the application of CLIRUN to the Yellow River in China.

Yates (1996) expanded on the basic CLIRUN by adding a snow-balance model and providing a suite of possible PET models and packaged it in a tool named WATBAL. WATBAL has been used on a wide variety of spatial scales from small to large watersheds and globally on a 0.5 by 0.5 degree grid (Strzepek et al. 1999; Huber-Lee et al., 2005; Strzepek et al. 2005).

CLIRUN-II (Strzepek et al. 2008) is the latest in the "Kaczmarek School" of hydrologic models. It incorporates most of the features of WATBAL and CLIRUN but was developed specifically to address extreme events at the annual level modeling low and high flows. CLIRUN and WATBAL did very well in modeling mean monthly and annual runoff, important for water supply studies, but was not able to accurately model the tails of runoff distribution.

CLIRUN-II has adopted a two-layer approach following the framework of the SIXPAR hydrologic model (Gupta and Sorooshian 1983, 1985). A unique conditional parameter estimation procedure was used. In the following section a brief description of the components of the model will be presented.

Spatial and Temporal Scale. CLIRUN-II models runoff as a lumped watershed with climate inputs and soil characteristics averaged over the watershed, simulating runoff at a gauged location at the mouth of the catchment. CLIRUN can run on a daily or monthly time step. For this study, climate and runoff data were available only on a monthly basis, so monthly was used.

Snow-Balance Model. The snow accumulation and melt model used in this study is based on concepts frequently used in monthly water balance models (McCabe and Wolock 1999). Inputs to the model are monthly temperature (T) and precipitation (P). The occurrence of snow is computed as a function of average watershed temperature and two parameters (Temp_snow and Temp_rain). These two parameters are calibrated for each watershed. Snowmelt is added to any monthly precipitation to form effective precipitation available for infiltration or direct runoff.

Water Balance. Figure A-1 is a schematic of the water flows of CLIRUN-II. The figure shows the mass balance of water in the CLIRUN-II system. Water enters via precipitation and leaves via evapotranspiration and runoff. The difference between inflow and outflow is reflected as change in storage in the soil or groundwater.

Figure A-1 CLIRUN-II Conceptual Hydrologic Model Schematic

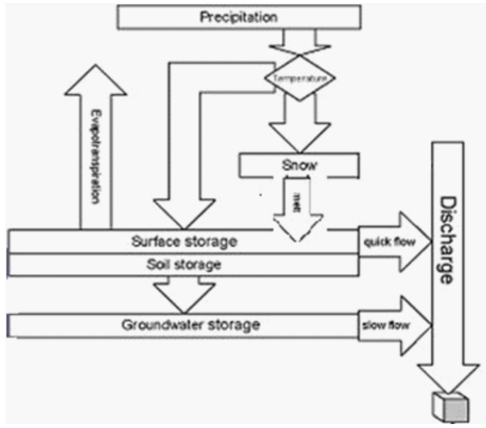

Evapotranspiration. A suite of potential evapotranspiration models are available for use in CLIRUN-II. For this study the modified Hargreaves method was used. Actual evapotranspiration is a function of potential evapotranspiration and soil moisture state following the FAO method (FAO 1996).

Soil Water Modeling. Soil water is modeled as a two layer system: a soil layer and groundwater layer. These two components correspond to a quick and a slow runoff response to effective precipitation.

Quick Runoff. The soil layer generates runoff in two ways. First there is a direct runoff component, which is the portion of the effective precipitation (precipitation plus snowmelt) that directly enters the stream systems. The remaining effective precipitation is infiltration to the soil layer. The direct runoff is a function of the soil surface and modeled differently for frozen soil and nonfrozen soil. The infiltration then enters the soil layer. A nonlinear set of equations determines how much water leaves the soil as runoff and how much is percolated to the groundwater and how much goes into soil storage. The runoff is a linear relation of soil water storage and percolation is a nonlinear relationship of both soil and groundwater storages.

Slow Runoff. The groundwater receives percolation from the soil layer and runoff is generated as a linear function of groundwater storage.

The soil water processes have six parameters similar to the SIXPAR model (Gupta and Sorooshian 1983) that is determined via the calibration of each watershed.

Modeling Dry & Wet Years

When CLIRUN-II is calibrated in a classical rainfall-runoff framework the results are very good for the 25th to 75th percentile of the observed streamflows, producing an R^2 value of 0.3 to 0.7 However, for most water resource systems the tails of the streamflow distribution are important for design and operation planning. To address this issue, a concept developed by Block and Rajagopalan (2008) for hydrologic modeling of the Nile River—known as localized polynomial—was extended to calibration of rainfall runoff modeling in CLIRUN-II (Strzepek et al. 2008).

When calibrating, each observed year is categorized as to whether it falls into a dry year 0 to 25 percent of the distribution, a normal year 25 percent to 75 percent, or wet year greater than 75 percent. A separate set of model parameters was estimated for the three different classes of annual streamflow. This increased the R^2 value from 0.7 to 0.92.

Runoff Results

The mean of the baseline runoff (1950–2000) was used to calculate a percent change in runoff for each basin and each of the four climate projections. Changes in runoff are expressed as percent deviation from the baseline. The time series of the changes in streamflow (cumulative runoff) for Gibe Omo and the Blue Nile are shown in Figure A-2 and A-3.

Figure A-2 Time Series of The Change In Annual Streamflow of The Gibe Omo For The Four Climate Projections

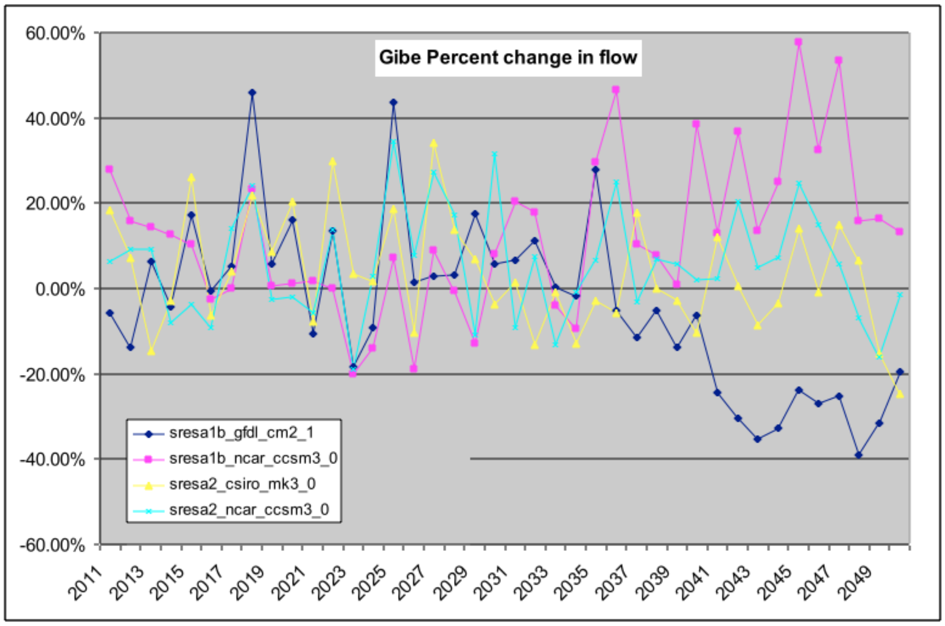

Figure A-3 Time Series of The Change In Annual Streamflow of The Blue Nile For The Four Climate Projections (Below)

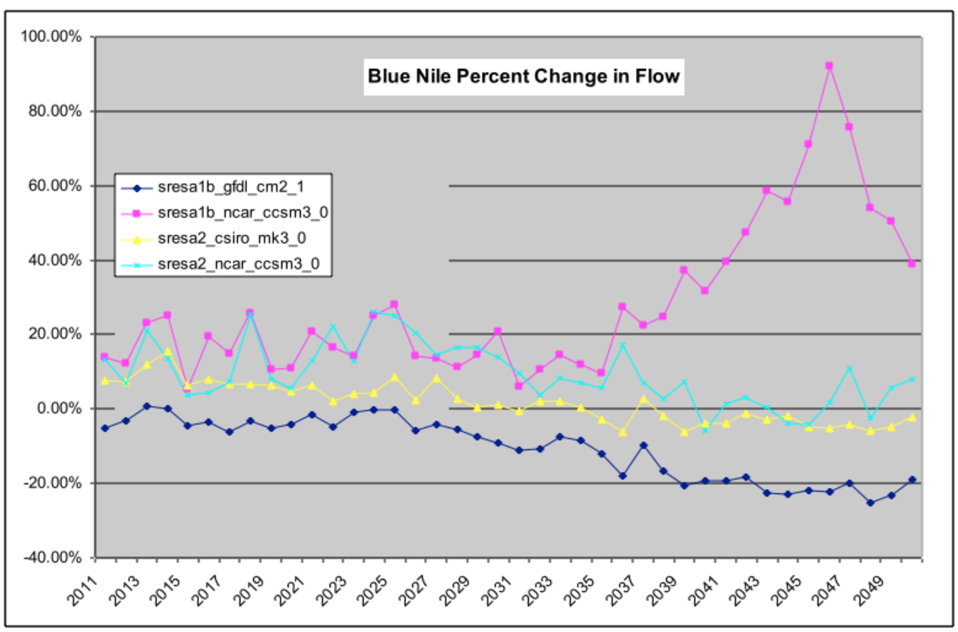

Annex 2
Cli-Crop Model

BACKGROUND

Crop models are used to predict future yields, estimate the effects of new agricultural management techniques on yields, and understand the effects of crop and soil type on food productivity and soil fertility. Many crop models have been developed over the last thirty to forty years in response to new research and more accessible computer technology. While crop simulators continue to be primarily used for academic purposes, farmers and policy makers are beginning to trust and use them.

The biggest question about crop modeling is whether or not crop models can predict future yields. Unfortunately, like most computer models of physical, chemical, or biological processes, the model's accuracy is heavily dependent on the model's input. All crop simulators require information on soil type, crop type, and weather, because these three factors have great effects on crop production. Soil parameters can be measured in a field one point at a time, but soil properties can change drastically on a small scale both vertically and horizontally. The growth of different crop types, which is based on complicated biological and chemical processes, also varies greatly by genotype geographic region, and even the individual plant. Weather, because of its chaotic behavior and dependence on both the large-scale and small-scale changes in the land and atmosphere, also continues to be very difficult to predict. In spite of these uncertainties, research in crop simulation continues because the human race is almost completely dependent on cultivated food. While crop models cannot deliver high-accuracy estimate of yields, they can provide insights on the impact of policy choices and farmers' decisions on crop yields.

There are many existing crop models. Each model has been built to solve a specific range of problems. The model's input and calculations depend on the input available and the accuracy that is required. For example, CropWat, a model developed by the Food and Agriculture Organization of the United Nations, is a very simple 1-dimensional crop model. CropWat requires very limited input and assumes no vertical differences in soil moisture, and assumes that the soil moisture cannot exceed field capacity. CropWat also simulates water stress on crops, ignoring any nutrient or solar stresses on a daily time-step. But CropWat is a tool to plan irrigation patterns for use by poor farmers in arid to semi-arid regions. So, CropWat does not need to calculate the effects of waterlogging or daily precipitation patterns. The model can assume that the farmer will irrigate and will not over-irrigate. SWAP, Soil-Water-Atmosphere-Plant, on the other hand, is a much more complicated soil moisture scheme, implementing Richard's equation on a time-step less than 30 minutes. SWAP requires more input and a faster computer, but models the movement of moisture in the soil layer using a more dynamic approach, allowing SWAT to claim more confidence in its solution.

CliCrop was developed because there were no existing models that the authors of this paper found to be adequate to solve certain problems. Specifically, these problems include modeling two water management techniques, zai holes and mulching, and also estimating the effects of climate change on crop yields, including both water stress from insufficient and excess water. The larger vision of CliCrop, which will continue beyond this paper, is that CliCrop can be a tool used to find agricultural techniques that could possibly offset the damages climate change may have on crop yields.

Originally, CliCrop was to be a modification of CropWat, and still, CropWat could be considered the base of CliCrop. But as CliCrop developed, it began to look less and less like CropWat.

CliCrop, as it stands now, maintains the same minimal input required by CropWat while reaching a more accurate yield estimation for both rainfed and irrigated agriculture.

In order to model the negative effects of waterlogging, a dynamic soil profile needed to be added to CropWat. This modification proved to be the most difficult. Many other crop models were reviewed for guidance, and some of their methods were borrowed for the development of CliCrop. Both the mathematics and the GUI were written in Matlab.

Structure of CliCrop

Figure A-4 below shows the modeling process as a whole. Each individual process is explained in detail in this chapter.

Figure A-4 Schematic of the CliCrop Model Procedure

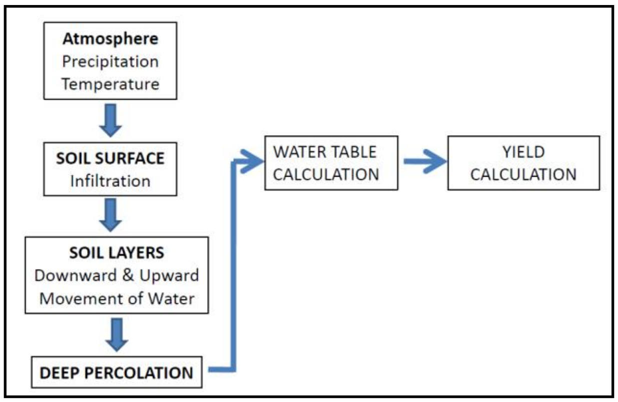

The effects of the atmosphere are modeled indirectly in the soil layer through the extraction of ET and the infiltration into the soil layers. The model uses the soil properties and precipitation amount to calculate the infiltration using the USDA Curve Number method. Then the model calculates the soil moisture in each soil layer. The model then calculates the amount of moisture allowed to percolate into the deep soil layers. The water table is then measured and a yield is calculated.

Input. CliCrop was designed for large-scale yield calculations, using both future and historical weather data and available soil data. Input into CliCrop is simple and the amount of required input is minimized in order to avoid as much error as possible involved with the input.

Precipitation. Since CliCrop runs on a daily timescale, total daily precipitation data is required in millimeters per day. The historic precipitation data that is currently built into the model comes from the collaborative historical African rainfall model (CHARM). The CHARM database contains 36 years (1961–96) of daily historic rainfall for all of Africa estimated by satellite and rain gauge data. (Funk et al. 2003)

Potential Evapotranspiration (ET). Potential evapotranspiration is a measurement of the atmosphere's ability to extract moisture from the soil both through evaporation and transpiration measured in mm/day. Table A-1 below shows the range of potential ET for different climatic regions (Allen et al. 1998)

Potential evapotranspiration is estimated based on a mean daily temperature, daily temperature range, and latitude. The modified Hargreaves equation (Hargreaves, ASCE, and Allen 2003) is used to find the potential ET based on these parameters.

Table A-1 Range of Potential ET

Average ET for different agroclimatic regions in mm/day

Regions	Mean daily temperature (°C)		
	Cool ~10°C	Moderate 20°C	Warm >30°C
Tropics & subtropics			
humid & sub-humid	**2 - 3**	**3 - 5**	**5 – 7**
arid & semi-arid	**2 - 4**	**4 - 6**	**6 - 8**
Temperate Region			
-humid & sub-humid	**1 - 2**	**2 - 4**	**4 – 7**
-arid & semi-arid	**1 - 3**	**4 - 7**	**6 - 9**

Crop Type

All of the crop parameters used by CliCrop were first developed by FAO in CROPWAT (Allen et al. 1998). CliCrop retrieves the crop parameters based on the crop specified by the user. These parameters include:

Single (time averaged) crop coefficients, K_c. These values are used in the calculation of actual and potential evapotranspiration. There are three coefficients for each crop. These values are used to create a coefficient for each day of the growing season (see table 12 in FAO Drainage Paper No. 56 in Allen et al. 1998)

Basal Crop Coefficient, K_{cb}. These values are only used to find the reduction in potential evapotranspiration caused by mulching. There are three coefficients for each crop similar to K_c. These values can be used to calculate actual and potential transpiration. (see Table 17 in FAO Drainage Paper No. 56 in Allen et al. 1998)

Crop Stage Durations. The length in days of each of the four stages in the growing season. These stages include the initial, development, middle, and final.

Yield Coefficients. Values used to weight the effect of water losses on the yield for each of the four stages of growth. These values are used in the yield calculation equation.

Root Growth Per Day. Roots will grow at this length (in mm) per day when growth is allowed.

Initial Root Depth. It is assumed that the root zone starts at an initial depth. This concept and value are both borrowed from CROPWAT and Irrigation and Drainage Paper No. 56 (Allen et al. 1998)

Growing Season Duration. Length of growing season in days. This value is the sum of the crop stage durations explained above.

Soil Properties

Estimations if Unknown is selected. The only soil properties required for CliCrop to run are hydraulic conductivity, wilting point, field capacity, and saturation. These parameters are estimated based on the location. A data set was acquired from the FAO Soil Map of the World that contains clay and sand content. The wilting point and field capacity are estimated based on methods developed by the National Center for Atmospheric Research (NCAR) (Oleson et al. 2004). A semi-impervious layer is assumed to be at a depth of 2 meters from the soil surface. The semi-impervious layer allows soil moisture to percolate at a rate of 1 percent the hydraulic conductivity when excess soil moisture exists in the bottom layer.

When either the Wise Soil Profile is used or the soil parameters are known, the model assumes a semi-impervious layer at the bottom on the soil profile, as described above. When the soil parameters are known, the model also assumes a semi-impervious layer at 2 meters.

Water Transport

Figure A-5 is a schematic diagram of the processes used by the model to solve for soil moisture in each soil layer. By default the model has 20 layers, each 10 cm deep. If the WISE soil profile is used, the number of layers is determined by the number of layers in the WISE soil profile.

Figure A-5 Schematic of the Soil Moisture Process Used by CliCrop

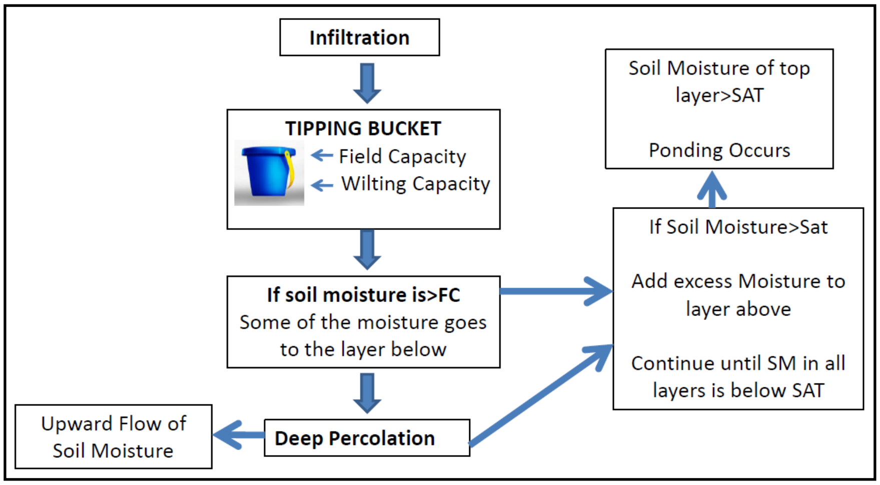

Once infiltration is calculated, the total amount of moisture infiltrated into the soil layer is added to the first layer. That layer is filled from wilting point to field capacity. Most of the moisture over field capacity is allowed to percolate to the layer below. The model then checks if the soil moisture in the layer is above saturation. If so, the model adds the moisture above saturation to the layer above until all moisture has found "space." If the top layer is saturated and excess soil moisture remains, the excess is considered lost to ponding. The model does this for each layer from the top to the bottom soil layer. At the bottom soil layer the model calculates deep percolation, which allows some of the moisture in the bottom soil layer to percolate past the semi-impervious layer. This moisture is considered lost to the deep soil layers. The model then checks one more time for any layer whose soil moisture is above saturation. Once all of this is finished, the model calculates the upward flow of soil moisture.

Effective Precipitation

Once the model retrieves the precipitation, the runoff is calculated based on the hydraulic conductivity of the first soil layer, the moisture content of the first soil layer, and the cover type using the National Resource Conservation Services' (NRCS) Curve Number Method. The curve number is estimated by a graph created by NRCS and printed in the Drainage Manual produced by the U.S. Interior Department's Bureau of Reclamation (Bureau of Reclamation 1993).

Evapotranspiration (ET)

The effective precipitation is then added to the moisture of the fist layer of the soil profile. CliCrop then calculates the soil moisture, one layer at a time, starting with the top layer and moving down to the bottom of the soil profile. During the dormant season, evaporation is removed from the top 12.5 cm of the soil profile using the following equations from FAO Irrigation and Drainage paper No. 56 (Allen et al. 1998)

Equation 1

$$TEW^{l} = (FC^{l} - 0.5 \cdot WP^{l}) \cdot delZ$$

$$K_{r}^{l,t} = \frac{SM^{l,t-1} - 0.5 \cdot (WP^{l} \cdot delZ)}{(1 - pe) \cdot TEW^{l}}$$

$$ETS^{l,t} = \frac{(ET0^{t} \cdot asm)}{nls0}$$

$$ETSA^{l,t} = ETS^{l,t} \cdot K_{r}^{l,t}$$

TEW^{l} = total evaporable water of layer l (mm)
FC^{l} = field capacity of layer l
WP^{l} = wilting point of layer l
delZ = thickness of layer l (mm)
$K_{r}^{l,t}$ = limiting coefficient of the evaporation for layer l at day t, $0 \le K_{r}^{l,t} \le 1$
$SM^{l,t-1}$ = soil moisture of layer l at the day before t (mm)
Pe = 0.4, fraction of TEW value for maximum evaporation
$ETS^{l,t}$ = maximum evaporation from layer l (mm)
$ET0^{t}$ = potential ET at day t (mm)
asm = 0.30, antecedent moisture coefficient; fraction of ET0 as evaporation
nls0 = number of layers in evaporation zone (top 12.5 cm)
$ETSA^{l,t}$ = soil moisture removed from layer l at time t due to evaporation (mm)

CliCrop contains two methods for determining ET: the single crop coefficient method and the dual crop coefficient method. If the single crop coefficient method is used, during the growing season, ET is removed from the root zone using the following equations from FAO Irrigation and Drainage paper No. 56 (Allen et al. 1998):

Equation 2

$$ETC^{l,t} = \frac{ET0^{t} \cdot K_{C}^{t}}{nlsr^{d}}$$

$$p = p_{tab} + 0.04 \cdot (5 - ETC^{l,t})$$

$$TAW^{l} = delZ \cdot (FC^{l} - WP^{l})$$

$$K_{s}^{l,t} = \frac{SM^{l,t-1} - WP^{l} \cdot delZ}{(1 - p) \cdot TAW^{l}}$$

$$ETA = K_{s}^{l,t} \cdot ETC^{l,t}$$

$ETC^{l,t}$ = crop specific ET demand (mm)
$ET0^{t}$ = potential ET at day t (mm)
K_{C}^{t} = crop coefficient at day t
$nlsr^{d}$ = number of layers in root zone
p = soil water depletion fraction
p_{tab} = soil water depletion fraction for no stress
(Listed in table 22 of FAO Irrigation and Drainage Paper No. 56)
TAW^{l} = total available water of layer l (mm)
delZ = thickness of layer l (mm)
FC^{l} = field capacity of layer l
WP^{l} = wilting point of layer l
$K_{s}^{l,t}$ = limiting coefficient for the calculation of actual ET for layer l at day t, $0 \le K_{r}^{l,t} \le 1$
$SM^{l,t-1}$ = soil moisture of layer l at the day before t (mm)
$ETA^{l,t}$ = soil moisture removed from layer l at time t due to ET (mm)

Figure A-6 shows a typical change in the crop coefficient, and therefore crop ET demand for the four development stages.

Figure A-6 Evolution of Crop Coefficient During the Growing Season

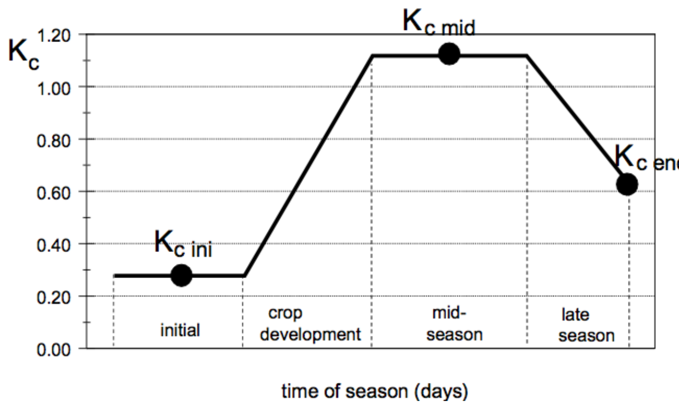

If the dual crop coefficient method is used, transpiration and evaporation are calculated separately during the growing season. In order to apply the changes made to transpiration caused by CO_2 fertilization, transpiration needs to be separated from evaporation. In general, this method was also taken from FAO Irrigation and Drainage paper No. 56 (FAO 56) (Allen et al. 1998). In this method a different crop coefficient was used: the basal crop coefficient (K_{cb}).

First, using a ratio of the precipitation and PET of the growing season, a climate classification method was used to find the minimum relative humidity (RH_{min}) for the growing season (Cazalac, PHI/UNESCO n.d.). Next, the crop height (h) is estimated based on the max crop height given in FAO 56 multiplied by a ratio of the crop specific demand of that day and the maximum crop specific demand. The crop height does not decrease, it only increases. Then K_{Cmax} (represents an upper limit on the evaporation or transpiration from any cropped surface) is calculated based on equation 72 in FAO 56, as shown below:

Equation 3
$$K_{Cmax} = \max\left(\left\{1.2 + [0.04(RH_{min} - 45)]\left(\frac{h}{3}\right)^{0.3}\right\}, \{K_{cb} + 0.05\}\right)$$

K_{Cmax} is then used to calculate the fraction of the ground covered by vegetation (f_c) using the equation below (equation 76 in FAO 56).

Equation 4
$$f_c = \left(\frac{K_{cb} - K_{c\min}}{K_{c\max} - K_{c\min}}\right)^{(1+0.5h)}$$

Where K_{cmin} is minimum K_c for dry bare soil, estimated to be 0.175 based on FAO 56. The fraction of soil surface that is moist, and therefore exhibits moist soil evaporation (f_{ew}) is calculated using the following equation, equation 75 from FAO 56.

Equation 5
$$f_{ew} = \min(1 - f_C, f_W)$$

Where f_W is taken from Table 20 in FAO 56, based on the type of irrigation, if any, that is used. Then a dimensionless evaporation reduction coefficient, K_r, is calculated using equation 74 in FAO 56 shown below.

Equation 6 $$K_r = \frac{TEW - D_{e,i-1}}{TEW - REW} \text{ for } D_{e,i-1} > REW$$

Where TEW is the total evaporable water (FC – 0.5*WP), REW is the readily available water and is calculated using Table 19 in FAO 56. $D_{e,i-1}$ is the cumulative depth of evaporation, calculated from the previous day. The soil evaporation coefficient, K_e, is calculated using equation 71 in FAO 56 shown below.

Equation 7 $$K_e = K_r(K_{C\max} - K_{cb})$$

The ET demand (ETC) is then calculated as:

Equation 8 $$ETC = \frac{(K_{cb} + K_e)ET_0}{nlsr}$$

And the actual ET removed from the soil layers is calculated the same as the single crop coefficient method, only using the above equation for ETC.

Soil Layer Percolation

Once ET is removed from the soil layer, percolation from the layer above is added based on the soil water excess equation borrowed from SWAT (Neitsch, Arnold et al. 2005).

Equation 9 $$TT = \left(\frac{SAT^l - FC^l}{HC^l}\right) \cdot delZ$$

$$SW_{excess}^{l,t} = SM^{l,t} - FC^l$$

$$Perc^{l,t} = SW_{excess}^{l,t} \cdot \left[1 - \exp\left(\frac{-\Delta t}{TT}\right)\right]$$

TT = travel time (hr)
SAT^l = moisture content at saturation of layer l
FC^l = moisture content at field capacity
HC^l = hydrualic conductivity (mm/hr)
delZ = thickness of layer (mm)
$SW_{excess}^{l,t}$ = soil water excess, $SW_{excess}^{l,t} \geq 0$ (mm)
$SM^{l,t}$ = soil moisture of layer l (mm)
$Perc^{l,t}$ = moisture to percolate to layer below (mm)
Δt = length of one time step (hrs)
Soil moisture is moved to the layer below only if the soil layer exceeds field capacity.

Ponding

After ET and percolation are removed, if the layer's soil moisture exceeds saturation, any soil moisture above saturation is added to the layer above until either all of the soil moisture has been placed, or ponding occurs at the soil surface. Any ponding is considered lost.

Deep Percolation

If percolation, as described above, continues to the bottom layer of the soil profile, deep percolation occurs. The most that is allowed to percolate out of the soil profile is 1 percent of the hydraulic conductivity per day. The rest is added to the layer above until either all layers have reached saturation (in which case ponding occurs), or until all moisture has been placed.

Soil Water Upward Flow

The following equations are used to estimate the movement of soil moisture against gravity. The method was borrowed from the DSSAT model (Ritchie 1998).

Equation 10

$$THET1 = SW(L) - LL(L)$$
$$THET2 = SW(L+1) - LL(L+1)$$
$$DBAR = (0.88 cm^2 day^{-1}) \times \exp(35.4 \times (THET1 \times 0.5 + THET2 \times 0.5)$$
$$FLOW = DBAR \times (THET2 - THET1) / ((DLAYR(L) + DLAYR(L+1)) \times 0.5)$$

THET1 = volumetric water content of layer L, changes daily (cm)
THET2 = volumetric water content of layer L+1, changes daily (cm)
SW = soil moisture, changes daily (cm)
LL = soil layers lower limit (cm)
DBAR = assumed average diffusivity (cm day^{-1})
FLOW = soil moisture moved from layer, L + 1, to layer, L
DLAYR = thickness of soil layer

Water Table

The water table is used to determine losses due to waterlogging. The height of the water table is measured from the bottom soil layer to the furthest saturated layer. If no layers are saturated, the height of the water table is considered to be zero. If the first layer is saturated, the height of the water table is equal to the depth of the soil profile. So, the height of the water table is not necessarily the height to which the soil is saturated. The water table height is independent of the moisture of all soil layers except the saturated layer closest to the surface.

Yield Reductions / Improvements and Adjustments to Crop Behavior Due to Climate

Yield calculations are based primarily on the ratio of actual ET and potential ET. Five yield values are calculated; one for each of the four development stages, and one for the whole season. The least of the five, considered the limiting yield, is reported as the true yield. Each yield value is calculated by the equation below, which was borrowed from the FAO Irrigation and Drainage Paper No. 56 (Allen, et al. 1998).

Equation 11

$$\left(1-\frac{Y_a}{Y_m}\right)=K_y^d\cdot\left(1-\frac{ETC^d}{ETA^d}\right)$$

$$\%Yield^d=\frac{Y_a}{Y_m}$$

Y_a = predicted actual yield
Y_m = maximum yield
K_y^d = yield coefficient, different for development stage d
ETC^d = sum of daily ET crop demand for development stage d
ETA^d = sum of daily actual ET for development stage d
$\%Yield^d$ = ratio of actual yield over maximum yield, value reported by CliCrop

Waterlogging

The reduction in yield due to waterlogging is simulated in CliCrop with two functions; an oxygen loss reduction coefficient, SEW_{30}, and the root growth hindrance.

SEW30. SEW_{30} was proposed by Sieben in 1964, and is a method to calculate waterlogging losses based on experimental data. SEW_{30} is a measurement of the magnitude and duration of the root zone's saturation.

Equation 12

$$SEW_{30}=\sum_{t=1}^{DUR}(30-x^t)$$

$$RY=\begin{cases}0.91-0.00031\cdot SEW_{30} & SEW_{30}>200\\ 1-0.00076\cdot SEW_{30} & \mathrm{SEW}_{30}\le 200\end{cases}$$

$$Yield=Yield_{wwl}-(1-RY)$$

SEW_{30} = sum of excess water, only calculated when the height of the water table is within 30 cm of the soil surface
t = day of growing season
DUR = duration of growing season
x^t = distance from soil surface to water table at day t
RY = reduced yield due to waterlogging
Yield = yield of season
$Yeild_{wwl}$ = yield without waterlogging losses
(Mohanty, et al. 1995)

Root Growth

When the watertable height is measured to be within the root zone, the roots are not allowed to grow for that day. This growth hindrance could cause yield reduction due to water losses for the crop in the future, since the roots may not be deep enough to access soil moisture in the deeper soil layers.

Zai Holes

Since there are no preceding models that have estimated the effect of zais on crop yields, and therefore no modeling process has been established or tried, the following is an attempt to simulate the process dynamically. The process was formed by the imagination of the creators of CliCrop. The effects of the zai holes are simulated with two separate soil profiles: catchment soil profile and zai hole soil profile. Both soil profiles have the same soil parameters; the only difference is the amount of effective precipitation that infiltrates into the profile. At the end of the growing season, the moisture in the soil profile is assumed to be an average of the two profiles for dormant season calculations. A diagram of the zai-hole modeling process is shown in Figure A-7.

Figure A-7 Diagram of the zai hole modeling process

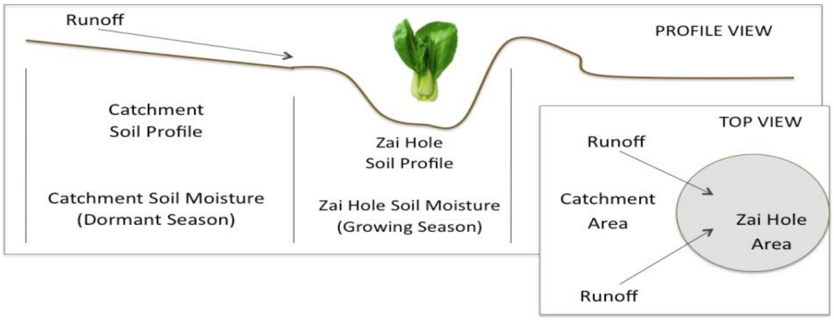

Catchment Soil Profile

The catchment soil profile is treated very similarly to the profile in the dormant season. Evaporation is removed (based on Irrigation and Drainage Paper No. 56) and the soil moisture transport between layers is calculated using the SWAT method. A water table height is not calculated because it is never used.

Zai Hole Soil Profile

The runoff from the catchment area is assumed to drain into the zai hole based on the catchment efficiency (determined by user). If the catchment efficiency is 100 percent, all of the runoff from the catchment enters the zai hole soil profile. If the catchment is 0 percent, only 50 percent of the runoff enters the zai hole soil profile and the other 50 percent is assumed lost. For any value in between 0 percent and 50 percent catchment efficiency, the runoff caught by the zai hole is calculated using a linear relationship.

Equation 13

$$\text{Runoff Caught} = \left(\frac{\text{Catchment Efficiency}}{2} + 50 \right) \cdot \mathit{Runoff} \cdot \text{Zai Ratio}$$

Runoff refers to the runoff from the catchment soil profile and Zai ratio is the zai area over the total area.

Mulching

None of the crop models that were studied prior to the construction of CliCrop included a process for modeling the effects of mulch on crop yields. But some research has been done on this topic and is used here. The effects of mulching are simulated in three separate ways: reduction in evapotranspiration, runoff reduction, and the organic matter increase.

Reduction in Evapotranspiration. Organic mulch has been proven to reduce the temperature at the soil surface, thus decreasing evapotranspiration. FAO Irrigation and Drainage Paper No. 56 proposed a simple method to mathematically simulate this reduction by reducing the crop coefficients based on the amount of ground that is covered by mulch.

Equation 14 $K_{C1}^{t}' = K_{C1}^{t} \cdot (1 - mulch/2)$

$$K_{C2}^{t}' = K_{C2}^{t} - mulch/2 \cdot (K_{C2}^{t} - K_{Cb2}^{t})$$

K_{C1}^{t}' = crop coefficient for the initial stage after reduction due to mulching
K_{C1}^{t} = crop coefficient for the initial stage before reduction due to mulching
mulch = percent of ground covered by organic mulch
K_{C2}^{t}' = crop coefficient for the middle stage after reduction due to mulching
K_{C2}^{t} = crop coefficient for the middle stage before reduction due to mulching
K_{Cb2}^{t} = basal crop coefficient for the middle stage
K_{C3}^{t}' = crop coefficient for the late stage after reduction due to mulching
K_{C3}^{t} = crop coefficient for the late stage before reduction due to mulching
K_{Cb3}^{t} = basal crop coefficient for the late stage

So, for every 10 percent of the ground that is covered by mulch, the crop coefficient is reduced by 5 percent. The crop coefficient for the initial stage is reduced much more than the second and third stages because the difference between the basal crop coefficient and the original one is usually fairly small. So, most of the benefit from ground cooling occurs at the beginning of the season (Allen et al. 1998).

Runoff Reduction. Runoff is reduced by organic mulch because the mulch causes more friction and an increase in the travel path. Due to a lack of available research on this phenomenon, a very simple method was chosen. When mulch is used, the curve number is reduced based on the following equation:

Equation 15 $CN' = CN - mulch \cdot 30$

CN' = reduced curve number due to organic mulching
CN = curve number before mulch reduction
mulch = % of ground covered by mulch

Adjustments to Crop Coefficients Due to Climate Changes

Whether the single crop coefficient method (K_c) or the dual crop coefficient method (K_{cb}) is used, the crop coefficients change due to changes in climate. This means that the crop's demand for water responds to changes in precipitation and potential ET FAO's Irrigation and Drainage Paper 56 suggests a method for adjusting these crop coefficients based on these weather changes. The CliCrop code adjusts these coefficients using the method presented by FAO 56 (Allen et al. 1998).

During the initial stage, the majority of ET is evaporation, while during the other three stages the majority of ET is generally transpiration. So the initial crop coefficient is calculated differently depending on whether the single or the dual crop coefficient method is used. If the single-crop coefficient method is used, the crop coefficient for the initial stage ($K_{C\ init}$) is calculated using the following equation.

Equation 16

$$t_W = \frac{L_{ini}}{n_W + 0.5}$$

$$E_{SO} = ET_0 \cdot 1.15$$

$$t_1 = REW / E_{SO}$$

$$K_{C\,\mathrm{ini}} = \frac{TEW - (TEW - REW)\exp\left(\frac{-(t_W - t_1 \cdot E_{SO}\left(1 + \frac{REW}{TEW - REW}\right))}{TEW}\right)}{t_W \cdot ET_0}$$

Where L_{ini} is the length of the initial stage; n_w is the number of wetting events in the initial stage; ET_0 is the average potential ET in the initial stage; REW is the readily available water estimated using the average wilting point of the soil, the average field capacity of the soil, and Table 19 from FAO 56; and TEW is the total evaporable water (FC – 0.5*WP). For the other two crop coefficients, $K_{c\,mid}$ and $K_{c\,end}$, the following equation is used.

Equation 17

$$K_c = K_c + 0.004(RH_{\min} - 45)\left(\frac{h}{3}\right)^{0.3}$$

Where the minimum relative humidity (RH_{min}) is calculated over the development stage, and mid-season stage, for $K_{c\,mid}$ and $K_{c\,end}$, respectively.

If the dual-crop coefficient method is used, the basal crop coefficients are estimated by the following equation.

Equation 18

$$K_{cb} = K_{cb} + 0.004(RH_{\min} - 45)\left(\frac{h}{3}\right)^{0.3}$$

Where the minimum relative humidity (RH_{min}) is calculated over the initial stage, development stage, and mid-season stage, for $K_{c\,ini}$, $K_{c\,mid}$, and $K_{c\,end}$, respectively.

Adjustments to Crop Stage Lengths Due to Climate Changes

The crop stage lengths also respond to changes in climate. As the temperature increases, the stage lengths shorten. The following equation was used to change all four of the crop stage lengths (Wahaj, Maraux, and Munoz 2007).

Equation 19

$$\Delta D_0 = \frac{D_0 \cdot \Delta T}{(T_{Ave} - T_{base})}$$

Where ΔD_0 is the change in the stage length (days) rounded to the nearest integer; D_0 is the original length of the crop stage, supplied as input; ΔT is the average change in temperature from the base temperature and the year of simulation during the given crop stage; T_{Ave} is the average temperature of the given crop stage; T_{base} is a crop specific parameter, supplied as input.

CO_2 Fertilization

Studies have shown that with increased CO_2 crop transpiration decreases due to increased stomatal resistance. In one such study, ratios are provided for C3 and C4 crops. CliCrop uses these ratios to reduce the transpiration demand as CO_2 increases using the following equations (Rosenzweig and Iglesias 1998).

Equation 20

$$CO_{2\,\mathrm{fert}} = \left[\left(\frac{SR - 1}{555 - 330} \right) (CO_2 - 330) + 1 \right]$$

$$T_{cb} = T_{cb} / CO_{2\,\mathrm{fert}}$$

Where SR is the stomatal resistance coefficient (for C3 crops SR = 49.7/34.4, and for C4 crops SR = 87.4/55.8); CO_2 is the amount of CO_2 in the atmosphere in parts per million; and T_{cb} is the crop transpiration demand.

Annex 3

Hydropower and the IMPEND Model

This annex describes an application of the expanded investment model for planning Ethiopian Nile development [IMPEND], including existing and planned national energy projects. Using global climate model (GCM) projections and trends (externally supplied), potential energy production is evaluated and compared with a no-climate-change simulation. Costs and timing of infrastructure development for adaptation are also evaluated. Subsequently, outputs are fed into a computable general equilibrium (CGE) model for further assessment.

Five simulations are evaluated in this project, including one base and four potential climate changes for the period 2010–50. The base embodies a no-climate-change trend, expressing only historical variability, representing one plausible projection. The GCMs and scenarios selected to produce potential climate change (Base historical variability with a trend) include GFDL a1b, NCAR a1b, CSIRO a2, and NCAR a2, representing the national driest and wettest and global driest and wettest respectively, as determined by the climate moisture index, from the suite of GCM ensemble members available. This is a reduced selection of potential simulations to provide a sense of potential sectoral changes. Relevant hydrologic and crop data for all simulations were externally assembled, downscaled, and supplied.

Energy Analysis

Existing and planned energy plants were drawn from the Ministry of Water Resources' Water Sector Development Plan (WSDP) and basin master plans and the Ethiopian Electric Power Corporation long-term development plans. The vast majority of these represent hydropower sources. Figure A-8 illustrates the approximate spatial location of hydropower plants; Table A-2 lists the baseline development plan, including anticipated power, year of commissioning, and project costs adjusted to 2010 U.S. dollars. As 2050 spans well beyond typical ministerial plans, best estimates are employed.

Figure A-8 **Existing and planned hydropower projects considered within Ethiopia**

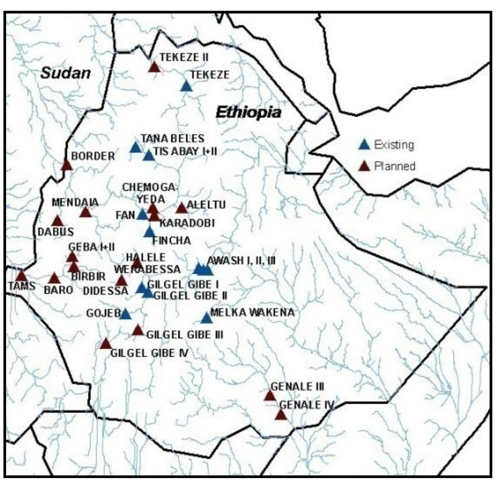

Table A-2 Assumed baseline energy development plan

Energy PlantExisting	Installed Capacity (MW)	Year of Commission	Cost ($M)
Awash I (Koka)	43	1960	
Awash II	32	1966	
Finchaa	134	1973	
Awash III	32	1974	
Melka Wakena	153	1988	
Tis Abay I & II	85	(1964) 2001	
Gilgel Gibe I	184	2004	
Gojeb (Independent)	150	2004	
Diesel & Geothermal	120		
Tekeze	300	2008	
Gilgel Gibe II	420	2008	
Tana Beles	460	2009	
Amerti-Neshi (FAN)	100	2010	
Fixed (committed)			
Wind - Ashegoba	120	2011	259
Gilgel Gibe III	1,870	2013	1730
Tendaho Geothermal	180	2013	305
Planned			
Gilgel Gibe IV	1,900	2014	2930
Halele Werabesa	450	2014	725
Chemoga-Yeda	278	2014	318
Geba I & II	366	2016	593
Genale III	258	2018	362
Genale IV	257	2018	456
Tekeze II	450	2020	694
Karadobi	1,600	2023	2411
Border	1,200	2026	1741
Mendaia	2,000	2030	2990
Baro	900	2034	914
Aleltu	405	2038	1444
Didessa	308	2038	523
Dabus	741	2042	1805
Birbir	467	2042	1199
Tams	1,060	2046	1805

The current version of IMPEND is a stand-alone energy model, written in GAMS, encompassing all basins within Ethiopia. The model is driven by monthly inputs of streamflow and net evaporation, which may vary from year to year, as prescribed by an input file. Hydropower reservoirs are assumed to operate at the design height, passing the full hydrograph of flows (no additional storage or releases.) Energy production commences upon the year of commission. Construction and capital costs are assumed divided over the five years prior to commissioning.

Figure A-9 presents anticipated total annual energy production under the base and four climate change scenarios considering the baseline development plan (Table A-2). Separation of the simulations becomes clearer in later decades. Generally, wetter (drier) simulations favor increasing (decreasing) energy production.

Summations of total energy production over the 40-year horizon are displayed in Table A-3. Also listed is the deficit or surplus resulting from each climate change simulation in comparison to the base simulation.

Figure A-9 Annual energy production for Base and four climate change scenarios

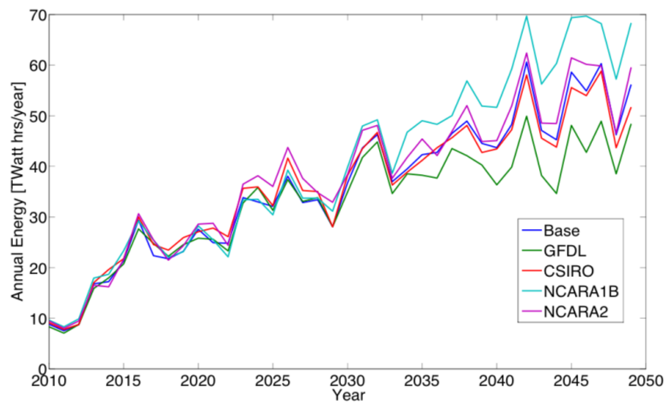

Table A-3 Summation of energy production over 40-year simulation for Base and climate change scenarios

Simulation	Total Energy (Twatt_hr/40yrs)	Difference with Baseline (Twatt_hr/40yrs)
Base	1435	-
GFDL A1B	1305	-130 (deficit)
NCAR A1B	1605	170 (surplus)
CSIRO A2	1440	5 (surplus)
NCAR A2	1515	80 (surplus)

Energy Adaptation Strategy

Adaptation strategies for the four climate change scenarios are founded on meeting or minimally exceeding annual energy production under the base simulation (utilizing the baseline development plan.) This is carried out by considering the same set of baseline development plants, in order, and shifting the year of commissioning as necessary to augment or reduce energy production. IMPEND is accordingly amended to handle the optimization routine.

Table A-4 presents the revised year of commission for each climate change simulation utilizing the IMPEND optimization routine. No changes in timing are allowed for the fixed (committed) projects through 2013. In some cases, particularly those favoring wetter conditions, project commissioning may actually lag baseline energy development, clearly presenting the opportunity for additional, unplanned energy production. This phenomenon is not exploited in this study. In other cases, plant commissioning must commence prior to the baseline development plan to meet or exceed annual energy production in a given year. For three of the simulations, additional, unplanned energy production beyond the final baseline energy plant (Tams) is required. Therefore, in any year post-commissioning of Tams, if the climate change simulation energy production falls below the base energy production, a "generic" project is amended to the development plan covering the difference.

As anticipated, simulations requiring projects to commence earlier than planned result in greater overall development costs when discounting is considered. Figure A-10 illustrates cumulative project costs discounted back to 2010 at a 5 percent rate. Generic project costs are based on existing and planned project power-cost relationships and values presented in current literature.

Table A-4 Project sequencing to meet or exceed baseline energy production

Energy Plant	Year of Commission				
Fixed (committed)	Base	GFDL A1B	NCAR A1B	CSIRO A2	NCAR A2
Wind - Ashegoba	2011	2011	2011	2011	2011
Gilgel Gibe III	2013	2013	2013	2013	2013
Tendaho Geothermal	2013	2013	2013	2013	2013
Planned					
Gilgel Gibe IV	2014	2013	2014	2014	2013
Halele Werabesa	2014	2014	2014	2015	2014
Chemoga-Yeda	2014	2015	2016	2015	2014
Geba I & II	2016	2015	2016	2016	2014
Genale III	2018	2016	2016	2018	2018
Genale IV	2018	2016	2018	2020	2018
Tekeze II	2020	2020	2019	2020	2018
Karadobi	2023	2020	2022	2020	2022
Border	2026	2023	2023	2026	2028
Mendaia	2030	2026	2030	2029	2030
Baro	2034	2030	2042	3031	2036
Aleltu	2038	2034	2047	2034	2036
Didessa	2038	2035	2047	2038	2039
Dabus	2042	2035	2047	2038	2042
Birbir	2042	2035	x	2039	2047
Tams	2046	2036	x	2042	2047
Annual shortfalls post-Tams project	-	6	-	5	1
Total energy shortfall (GW_hrs/yr)	-	12,130	-	4,470	460

Table A-5 Summation of discounted (2010) hydropower project costs over 40-year simulation for base and climate change scenarios

	Total Cost (Billion $)		Difference with Baseline (Billion $)	
Simulation	0% discount	5% discount	0% discount	5% discount
Base	22.8	12.4	-	-
GFDL A1B	25.2	14.4	2.4	2.0
NCAR A1B	19.8	11.6	-3.0	-0.8
CSIRO A2	23.7	13.1	0.9	0.7
NCAR A2	22.9	12.4	0.1	0

Figure A-10 Cumulative discounted project costs at 5% for base and four climate change scenarios

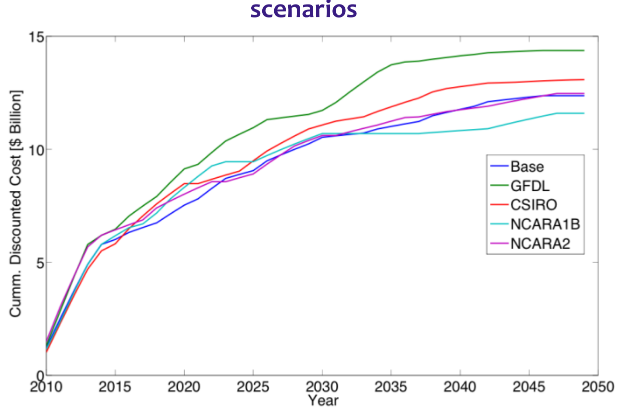

Table A-5 outlines total development costs for the base and climate change simulations in 2050, including expected differences between them. The GFDL model simulation (drying) projects a $2.4 billion overrun while the NCAR a1b model projects a $3 billion savings; the remaining two simulations tend closer to the base.

Annex 4
WEAP21 Model Description

This model description was taken from SEI-US Center's WEAP website (weap21.org). More detailed information can be found in the user guide (http://weap21.org/index.asp?doc=08).

WEAP is a microcomputer tool for integrated water resources planning that attempts to assist rather than substitute for the skilled planner. It provides a comprehensive, flexible, and user-friendly framework for planning and policy analysis. A growing number of water professionals are finding WEAP to be a useful addition to their toolbox of models, databases, spreadsheets, and other software. This introduction presents WEAP's purpose, approach, and structure; a detailed technical description of WEAP capabilities is available in a separate publication, the WEAP User Guide.

BACKGROUND

Many regions are facing formidable freshwater management challenges. Allocation of limited water resources, concerns regarding environmental quality, planning under climate variability and uncertainty, and the need to develop and implement sustainable water use strategies are increasingly pressing issues for water resource planners. Conventional supply-oriented simulation models are not always adequate for exploring the full range of management options.

Over the last decade, an integrated approach to water development has emerged that places water supply projects in the context of demand-side management, as well as water quality and ecosystem preservation and protection. WEAP incorporates these values into a practical tool for water resources planning and policy analysis. WEAP places demand-side issues such as water use patterns, equipment efficiencies, re-use strategies, costs, and water allocation schemes on an equal footing with supply-side topics such as streamflow, groundwater resources, reservoirs, and water transfers. WEAP is also distinguished by its integrated approach to simulating both the natural (e.g., evapotranspirative demands, runoff, baseflow) and engineered (e.g., reservoirs, groundwater pumping) components of water systems, allowing the planner access to a more comprehensive view of the broad range of factors that must be considered in managing water resources for present and future use. The result is an effective tool for examining alternative water development and management options.

WEAP operates in many capacities:

Water balance database. WEAP provides a system for maintaining water demand and supply information.

Scenario generation tool. WEAP simulates water demand, supply, runoff, streamflows, storage, pollution generation, treatment, and discharge and instream water quality.

Policy analysis tool. WEAP evaluates a full range of water development and management options, and takes account of multiple and competing uses of water systems.

The WEAP Approach

WEAP operates on the basic principle of a water balance and can be applied to municipal and agricultural systems, a single watershed, or complex transboundary river basin systems. Moreover, WEAP can simulate a broad range of natural and engineered components of these systems, including rainfall runoff, baseflow, and groundwater recharge from precipitation; sectoral demand analyses; water conservation; water rights and allocation priorities; reservoir operations; hydropower generation; pollution tracking and water quality; vulnerability assessments; and ecosystem requirements. A financial analysis module also allows the user to investigate cost-benefit comparisons for projects.

The analyst represents the system in terms of its various supply sources (e.g., rivers, creeks, groundwater, reservoirs, and desalination plants); withdrawal, transmission, and wastewater treatment facilities; water demands; pollution generation; and ecosystem requirements. The data structure and level of detail can be easily customized to meet the requirements and data availability for a particular system and analysis.

WEAP applications generally include several steps.

Study Definition. The time frame, spatial boundaries, system components, and configuration of the problem are established.

Current Accounts. A snapshot of actual water demand, pollution loads, resources, and supplies for the system are developed. This can be viewed as a calibration step in the development of an application.

Scenarios. A set of alternative assumptions about future impacts of policies, costs, and climate, for example, on water demand, supply, hydrology, and pollution can be explored. (Possible scenario opportunities are presented in the next section.)

Evaluation. The scenarios are evaluated with regard to water sufficiency, costs and benefits, compatibility with environmental targets, and sensitivity to uncertainty in key variables.

Examples of WEAP Scenario Analyses

Scenario analysis is central to WEAP. Scenarios are used to explore the model with an enormous range of "what if" questions, such as:

- What if population growth and economic development patterns change?
- What if reservoir operating rules are altered?
- What if groundwater is more fully exploited?
- What if water conservation is introduced?
- What if ecosystem requirements are tightened?
- What if a conjunctive use program is established to store excess surface water in underground aquifers?
- What if a water recycling program is implemented?
- What if a more efficient irrigation technique is implemented?
- What if the mix of agricultural crops changes?
- What if climate change alters demand and supplies?
- How does pollution upstream affect downstream water quality?
- How will land use changes affect runoff?

WEAP Development

The Stockholm Environment Institute provided primary support for the development of WEAP. The Hydrologic Engineering Center of the U.S. Army Corps of Engineers funded significant enhancements. A number of agencies, including the UN, World Bank, USAID, US EPA, IWMI, AwwaRF and the Global Infrastructure Fund of Japan have provided project support. WEAP has been applied in water assessments in dozens of countries, including the United States, Mexico, Brazil, Germany, Ghana, Burkina Faso, Kenya, South Africa, Mozambique, Egypt, Israel, Oman, Central Asia, India, Sri Lanka, Nepal, China, South Korea, and Thailand.

Annex 5

CGE Model: Additional Data & Information

Table A-6 **Aggregation of Activities, Commodities, and Households**

Activities	In Zones	Commodities	
atef	2 3 4	**Ctef**	Teff
awhea	2 3 4	**Cwheat**	Wheat
amaiz	1 2 3 4 5	**Cmaize**	Maize
abarsor	1 2 3 4 5	**Cbarsor**	Barley and sorghum
aenset	1 2 3 4	**Cagex**	Export agriculture
aagex	1 2 3 4 5	**Censet**	Enset
aothrag	1 2 3 4 5	**Cothrag**	Other agricultural products
alivst	1 2 3 4 5	**Clivstk**	Livestock
		Chome1	Home-produced agricultural products
		Chome2	Home-produced processed food and services
Amilling		**Cmilling**	Flour and milling services
Afood		**Cfood**	Other processed food, beverages, tobacco
Achem		**Cchem**	Chemicals
Aelect		**Celect**	Electricity
Awater		**Cwater**	Water
		Cptrl	Petrol
Ai-mfg		**Ci-mfg**	Intermediate and investment goods
Af-mfg		**Cf-mfg**	Final consumer goods
Aconst		**Cconst**	Construction services
Atrd-trn		**Ctrd-trn**	Trade and transport services
Agov		**Cgov**	Public admin, education, health services
Aosvc		**Cosvc**	Other services
Factors			
flab0	Agricultural labor		
flab12	Administrative workers and professionals		
flab3	Unskilled workers		
flab4	Skilled workers		
fland1	Land - Zone 1		
fland2	Land - Zone 2		
fland3	Land - Zone 3		
fland4	Land - Zone 4		
fland5	Land - Zone 5		
flvstk1	Livestock capital - Zone 1		
flvstk2	Livestock capital - Zone 2		
flvstk3	Livestock capital - Zone 3		
flvstk4	Livestock capital - Zone 4		
flvstk5	Livestock capital - Zone 5		
fkptl	Capital		

Table A-7 Household Income by Source (Shares)

	Base	Labo	Lab12	Lab3	Lab4	Land	Livstk	Cap	GovTr	RoWTr	Total
HH-Rural_EZ1P	*0.510*	0.77	0.00	0.00	0.00	0.04	0.05	0.11	0.03	0.00	1.00
HH-Rural_EZ2P	*9.857*	0.73	0.00	0.00	0.00	0.04	0.07	0.13	0.01	0.03	1.00
HH-Rural_EZ3P	*4.651*	0.68	0.02	0.00	0.00	0.04	0.04	0.14	0.02	0.06	1.00
HH-Rural_EZ4P	*8.423*	0.64	0.01	0.00	0.00	0.03	0.05	0.20	0.02	0.05	1.00
HH-Rural_EZ5P	*1.544*	0.12	0.00	0.00	0.00	0.02	0.33	0.45	0.01	0.08	1.00
HH-Rural_EZ1NP	*0.732*	0.46	0.01	0.00	0.00	0.04	0.04	0.43	0.00	0.01	1.00
HH-Rural_EZ2NP	*32.532*	0.41	0.02	0.00	0.00	0.11	0.05	0.39	0.00	0.02	1.00
HH-Rural_EZ3NP	*13.537*	0.39	0.03	0.00	0.00	0.12	0.03	0.41	0.01	0.02	1.00
HH-Rural_EZ4NP	*25.014*	0.35	0.01	0.00	0.00	0.10	0.04	0.45	0.01	0.05	1.00
HH-Rural_EZ5NP	*3.693*	0.07	0.00	0.00	0.00	0.01	0.19	0.66	0.01	0.07	1.00
HH-smallurbanP	*2.819*	0.00	0.08	0.20	0.48	0.00	0.00	0.10	0.05	0.09	1.00
HH-BigurbanP	*1.869*	0.00	0.14	0.06	0.33	0.00	0.00	0.10	0.03	0.33	1.00
HH-smallurbanNP	*15.674*	0.00	0.10	0.06	0.25	0.00	0.00	0.49	0.02	0.07	1.00
HH-BigurbanNP	*13.431*	0.00	0.09	0.03	0.25	0.00	0.00	0.28	0.03	0.33	1.00

Table A-8 Commodity Structure of Production, Trade, and Consumption (Below)

	Share in Domestic Production	Share in Total Imports	Share in Total Exports	Share of Exports in Output	Share of Imports in Dom. Demand	Share in Household Consumption	Share in Rural Poor Consumption
Ctef	0.012	0.000	0.000	0.000	0.000	0.017	0.007
Cwheat	0.009	0.035	0.000	0.000	0.492	0.023	0.038
Cmaize	0.009	0.000	0.000	0.001	0.001	0.013	0.024
Cbarsor	0.010	0.000	0.000	0.002	0.000	0.014	0.022
Cagex	0.041	0.001	0.336	0.726	0.020	0.029	0.029
Censet	0.004	0.000	0.000	0.000	0.000	0.006	0.009
Cothrag	0.037	0.011	0.043	0.105	0.079	0.058	0.058
Clivstk	0.051	0.002	0.047	0.082	0.009	0.065	0.046
Chome1	0.121	0.000	0.000	0.000	0.000	0.197	0.289
Chome2	0.088	0.000	0.000	0.000	0.000	0.143	0.195
Cmilling	0.008	0.002	0.015	0.167	0.069	0.009	0.008
Cfood	0.031	0.033	0.033	0.096	0.230	0.056	0.043
Cchem	0.009	0.123	0.019	0.200	0.818	0.042	0.036
Celect	0.008	0.000	0.000	0.000	0.000	0.005	0.000
Cwater	0.006	0.000	0.003	0.051	0.001	0.003	0.001
Cptrl	0.000	0.122	0.000	-	1.000	0.010	0.006
Ci-mfg	0.021	0.092	0.034	0.148	0.568	0.012	0.007
Cf-mfg	0.031	0.336	0.068	0.201	0.776	0.122	0.069
Cconst	0.113	0.000	0.000	0.000	0.000	0.000	0.000
Ctrd-trn	0.184	0.173	0.295	0.144	0.216	0.025	0.010
Cgov	0.108	0.002	0.008	0.006	0.004	0.033	0.020
Cosvc	0.100	0.068	0.097	0.087	0.020	0.118	0.083
ToT (Avg)	*1.000*	*1.000*	*1.000*	*0.090*	*0.133*	*1.000*	*1.000*
AgFood	*0.421*	*0.084*	*0.475*	*0.101*	*0.053*	*0.631*	*0.769*

Annex 6
WEAP Intersectoral Analysis Data & Methods

Surface Water

Surface water inflow was modeled with the rainfall-runoff model CLIRUN-II, which is the latest model in a family of hydrologic models developed specifically for the analysis of the impact of climate change on runoff (Strzepek et al. 2008). More information about CLIRUN-II can be found in the Annex 1. The historical time series of unmanaged surface water flow—that is, if all management (storage, diversions, etc.) were removed, unmanaged flow would remain—was calculated by CLIRUN-II for the 21 basins and used as the historical surface water that is available in each basin. The unmanaged flow from CLIRUN-II is the amount that enters the aggregated reservoir or the aggregated river if no reservoir is being modeled. CLIRUN-II was calibrated to historical basin outflows.[1] Future surface water flows based on the four Ethiopia climate change scenarios were calculated by CLIRUN-II for each of the 21 basins between 2001 and 2050. Figure A-11 provides flows under baseline and climate change conditions. As expected, the Ethiopia dry and wet scenarios represent the lower and upper bound projections on runoff.

Figure A-11 Total Annual CLIRUN Inflows for Ethiopia under the Baseline and Four Climate Change Scenarios, 2001–50

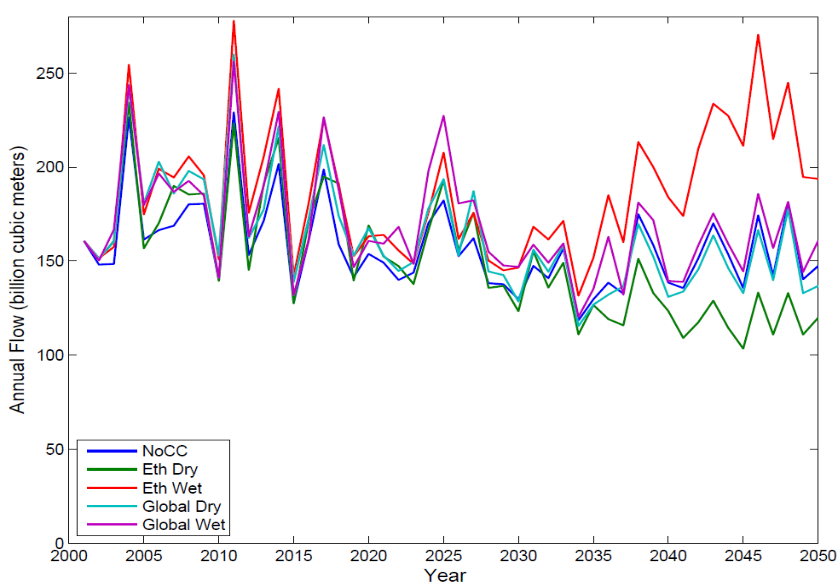

[1] As noted above, this analysis aggregates the flows to one inflow location so that all demands have access to all the water in the basin. Directly linking individual demands and supply is beyond the scope of this analysis. Because reservoirs have access to the entirety of the lumped flow in each basin rather than the flow from the reservoir catchment only (i.e., a smaller area), the analysis may overestimate the volume of water available for storage and hydropower generation.

Reservoirs and Hydropower

Reservoir storage and locations were determined using data from Block (2010) and from FAO's Africa Dams Database (2005). All existing storage capacity as of 2000 was aggregated in each basin to make one aggregate reservoir. If no storage was reported in a basin, then the modeled reservoir is assumed to have zero storage capacity. In many instances, reservoir volume data were missing but reservoir surface areas and generation capacities were available. To address this, an exponential curve was fit to available surface area and volume data, and this relationship was used to predict reservoir volumes (following Wiberg and Strzepek 2003). The equation had an R-squared value of 0.57.

Table A-9 provides a list of storage and hydropower capacity in the four basins with storage projects reported by Block and FAO in 2000. Following Block (2010), hydropower plants were assumed to run 24 hours per day and be 50 percent efficient. To convert from MW to MWh, the MW value was therefore multiplied by 8,760 for conversion to hours and by 0.5 for efficiency.

By 2050, the Ethiopian government projects a much larger amount of hydropower will be in place. In WEAP, these additional reservoirs are added as separate nodes with separate operational characteristics. Table A-10 presents the storage capacity and hydropower projected in Ethiopia in 2050. In total, storage volume is projected to rise over 10-fold, and hydropower capacity is projected to increase by almost 50-fold.

Table A-9 Storage Capacity, Hydropower Capacity, and Hydropower Generation in the 21 Basins in 2000

Subbasin	Storage (MCM)	Hydropower Capacity (MW)	Assumed Hydropower Generation (MWH)
Akoba	75	0	0
Awash Wenz 2	1,945	107	468,660
Blue Nile 4	775	134	586,920
Blue Nile 5	5	85	372,300
Total	2,800	326	1,427,880

Table A-10 Storage Capacity, Hydropower Capacity, and Hydropower Generation in the 21 Basins in 2050

Subbasin	Storage (MCM)	Hydropower (MW)	Assumed Hydropower Generation (MWH)
Akoba	75	0	0
Awash Wenz 2	1,945	512	2,242,560
Baro Wenz	528	1,733	7,590,540
Blue Nile 2	864	1,200	5,256,000
Blue Nile 4	2,222	4,112	18,010,560
Blue Nile 5	5	545	2,387,100
Dabus Wenz	745	741	3,245,580
Ghenale	23,365	4,285	18,768,300
Jema Shet	44	405	1,773,900
Omo	1,947	1,512	6,622,560
Tekeze Wenz	73	750	3,285,000
Total	***31,813***	***15,795***	***69,182,100***

Municipal and Industrial Demand

M&I water demand per capita for Ethiopia was provided by Hughes et al. (2009). For 2000, these values are 5.35 and 0.36 cubic meters per year for per capita municipal and industrial demands. Absent specific information on the distribution of water use across Ethiopia, M&I demands are assumed to be directly proportional to population. National water demand estimates are allocated to Ethiopia basins using a gridded population of the world dataset (CIESIN 2010), which provides gridded population data at five minute by five minute resolution (i.e., roughly 8 km x 8 km). Because rural populations with undeveloped water systems are likely to consume less water per capita, our averaging approach underestimates demand for water in urban areas such as Addis Ababa, and overestimates water demand in the rural areas. Table A-11 provides the population in each basin and the implied municipal and industrial demands in year 2000. It was assumed that the M&I demands consume 15 percent of their water intake; the remainder goes back to the river (Postel et al. 1996). In the WEAP model, the M&I demands are given a level 1 priority so that these demands are met before hydropower or irrigation.

Table A-11 Basin Population in 2000 and Municipal and Industrial Demands

Basin	Population	Municipal Demand (m^3)	Industrial Demand (m^3)
Akoba	590,795	3,162,796	213,352
Alal	34,659	185,546	12,516
Awash Wenz 1	167,834	898,492	60,609
Awash Wenz 2	8,266,470	44,254,202	2,985,243
Baro Wenz	1,675,890	8,971,807	605,209
Blue Nile 4	5,058,530	27,080,629	1,826,770
Blue Nile 2	526,043	2,816,149	189,968
Blue Nile 3	98,034	524,821	35,403
Blue Nile 5	6,478,700	34,683,450	2,339,631
Dabus Wenz	769,789	4,121,033	277,991
Dawa	966,731	5,175,354	349,112
Didesa Wenz	2,205,670	11,807,962	796,526
Ghenale	1,701,950	9,111,318	614,620
Jema Shet	1,862,600	9,971,351	672,635
Juba 2	65,318	349,677	23,588
Lake Abaya	4,006,430	21,448,256	1,446,829
Lake Turkana	1,034,950	5,540,562	373,748
Lakes Shala / Zeway	3,078,190	16,478,962	1,111,616
Omo	6,879,460	36,828,902	2,484,356
Tekeze Wenz	4,650,790	24,897,810	1,679,524
White Nile 5	18,210	97,486	6,576
Total	***50,137,043***	***268,406,564***	***18,105,823***

In future years, both population and M&I demand per capita will increase. Hughes et al. (2009) provide a projection of these increases every five years from 2005 to 2050 (2000 estimates are from CIESIN). In the absence of spatially disaggregated population projections (e.g., broken down by administrative regions), this analysis assumes that increases in population are distributed across basins proportionately based on the population distribution in 2000. Data needed to refine this assumption, such as past migration and urbanization, as well as projections of future migration, were unavailable for this study. Figure A-12 presents the increase in population, municipal per capita demand, and industrial per capita demand. Population is projected to rise roughly threefold between 2000 and 2050, and per capita demand is projected to increase by a factor of 2.5. Collectively, these two rising factors generate significant percentage increases in M&I water demand, although for perspective, total 2050 M&I withdrawals remain far lower than total irrigation withdrawals.

Figure A-12 Population and Per Capita Water Use Projections for Ethiopia, 2000–50

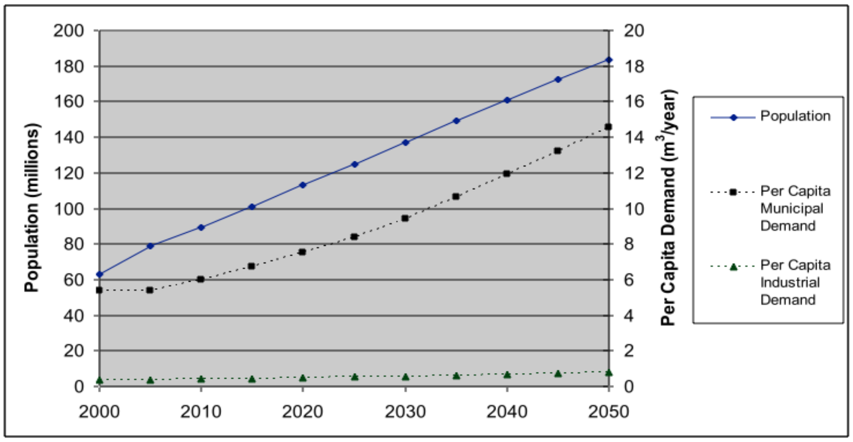

Irrigation Demand

Year 2000 irrigated area was based on an IFPRI database of irrigated hectares by crop for the administrative regions and zones of Ethiopia, which was provided by Block (2010). Using GIS software, these irrigated areas at the administrative level were interpolated to the basin level. The base irrigated area is provided in Figure A-13. IFPRI data indicates that a total of approximately 160,000 ha were irrigated in 2000 of the 10 million ha in Ethiopian agriculture (i.e., only 1.6 percent of agricultural land was irrigated). Of these 160,000 ha, approximately 130,000 ha were contained within the 21 basins that are the focus of this analysis. The three basins with the highest concentration of irrigated areas are Awash Wenz 2, Blue Nile 4, and Blue Nile 5.

Figure A-13 Base Irrigated Area in Each Basin

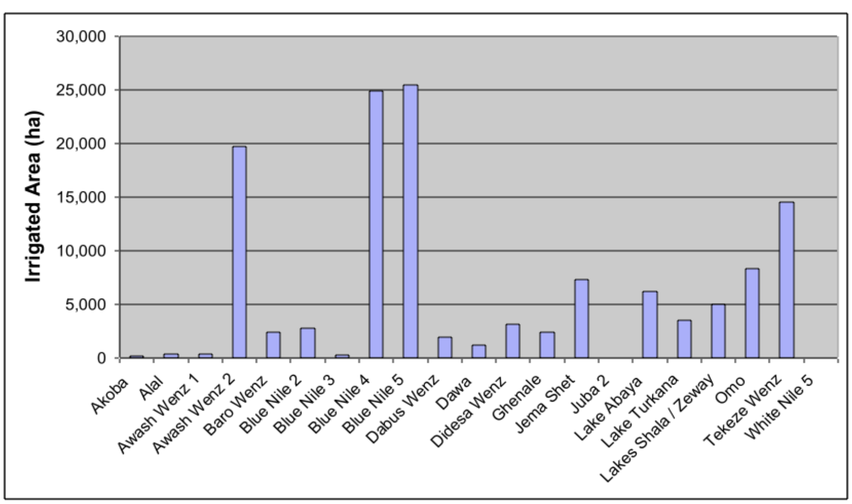

Annual water use per hectare for Ethiopia was provided by AQUASTAT (FAO 2000), which indicated that irrigation withdraws 2.47 km^3 of water per year for 161,000 ha equipped for irrigation in 2000. This converts to 15,342 m^3 per ha. Aquastat also indicates that of these countrywide withdrawals, biophysical crop water demand is only 0.56 km^3, implying an irrigation efficiency of 22.7 percent. This analysis rounds that efficiency to 25 percent starting in 2000. This initial efficiency is supported by the findings in a study by Bekele and Tilabun (2006). As more efficient irrigation technologies are adopted, the analysis assumes that irrigation efficiency increases from poor to good (FAO 1989) linearly to 50 percent by 2050 (i.e., the other 50 percent returns to the river). Consequently, because crop water demands remain constant, withdrawals per hectare fall to one-half of their 2000 values by 2050. Although increased efficiency as modeled has no effect on downstream flows because it causes proportionately lower return flows, reduced irrigation withdrawals ease upstream reservoir release requirements and thus reduce potential hydropower conflicts on a per hectare basis.

Monthly irrigation withdrawals over a typical year are included in the model, which is driven by crop water demands. Based on a case study of Ethiopian agriculture by van den Ham (2008), it is assumed that the crop being irrigated in Ethiopia is a second-season crop. According to van den Ham, typical second-season water withdrawals in his study area are concentrated in March through May and November. This pattern of withdrawals is adopted, and coupled with the total annual irrigation volumes per hectare from AQUASTAT to generate the monthly water demands in Figure A-14.

Figure A-14 Assumed Monthly Irrigation Withdrawals in Ethiopia

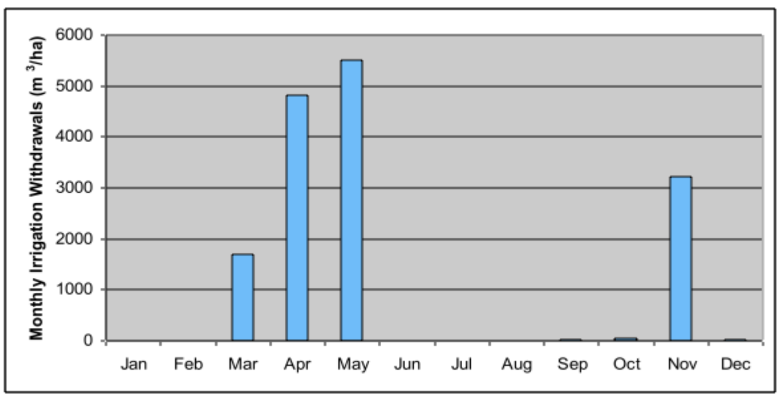

Following the approach of Block (2010), this analysis assumes that irrigated areas increase to 600,000 ha by 2010, 775,000 ha by 2016, and 3.7 million ha by 2050, without including any additional irrigation needed to respond to climate change. Block found that an additional 300,000 to 400,000 ha of additional irrigation will be needed to maintain constant yields under climate change, so the analysis also considers a scenario in which 4.1 million ha of land are irrigated. These increases are distributed proportionately within each basin according to the pattern of irrigation in 2000 presented in Figure A-13. This assumption is made in lieu of irrigation planning documents.

Transboundary Flow Requirements

Given the current status of negotiations among countries on the Nile and in other Ethiopia basins, it was impossible for this analysis to make any assumptions about border flow requirements on rivers flowing out of Ethiopia. Instead, this analysis tracks annual Ethiopian outflows under the growth scenario relative to unmanaged outflows. This provides a notion of the significance of growing Ethiopian demands for downstream countries' supplies. Block (2010) identified reservoir fill-time as a potentially important factor in determining the economic feasibility of planned hydropower facilities and can substantially diminish a river's flow for several years.

Annex 7
Livestock Model Transfer Approach and Assumptions

Step 1. Develop baseline livestock choice probabilities within each AEZ

It was assumed that the baseline probability of choosing a particular livestock type as a farm's primary animal is revealed through the existing distribution of livestock types, measured in tropical livestock units (TLU), in each AEZ. In order to generate the percentages of each livestock type at the AEZ level, data were first gathered on livestock counts in Ethiopian regions and zones from the International Livestock Research Institute (ILRI) and FAO. ILRI (2007) provides a GIS shapefile of the distribution of cattle, goats, and sheep across Ethiopia in 1999; the data for cattle are presented spatially in Figure A-15. These data were distributed spatially to the AEZ level with GIS, using interpolation where necessary.

Figure A-15 Distribution of Cattle Across Ethiopia in 1999

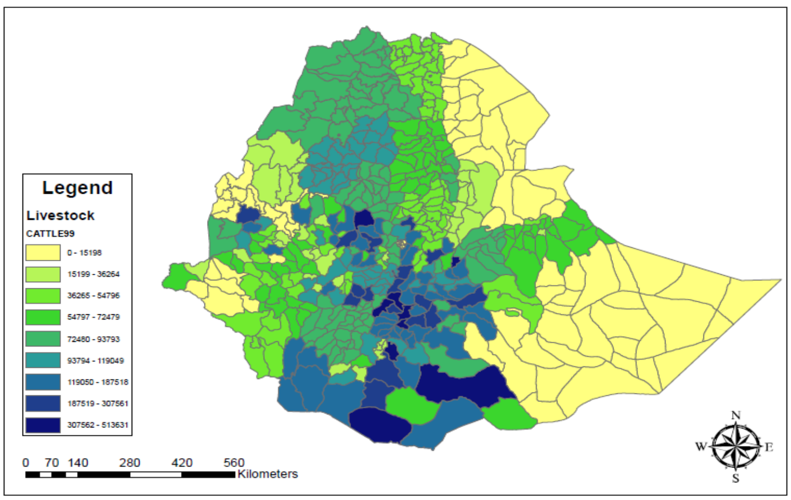

Source: ILRI (2007)

The ILRI data do not contain information on the number of chickens or on the breakdown of beef versus milk cattle, so the analysis relies on other sources. For the breakdown on beef versus milk cattle, Kedija et al. (2008) indicate that there are roughly 43 million cattle in Ethiopia, of which approximately 10 million (23 percent) are for milk production. FAOSTAT provides the year 2000 total number of cattle, goats, sheep, and chickens across Ethiopia; the current analysis uses the ratio of chickens to the sum of cattle, sheep, and goats (all in TLUs) to transfer the data into the ILRI dataset, and assumes that ratio was constant across AEZs.

Different livestock types are brought onto a comparable scale (i.e., to be able to compare cattle and chickens) using the TLU conversions from FAO (specifically, from Otte and Chilonda 2002). On this scale, a TLU of 1.0 is an animal weighing 250 kg; cattle are 0.7 TLU, sheep and goats each are 0.1 TLU, and chickens are 0.01 TLU. The overall number of livestock from the above steps are converted to TLUs. These values are presented in Table A-12 below, and are taken to be the baseline probabilities of choosing each livestock type in each Ethiopian AEZ.[2]

Table A-12 Distribution of TLUs by Livestock Type Across AEZs in Ethiopia (%)

AEZ	Beef Cattle	Cows	Goats	Sheep	Chickens
1	64.1	19.4	10.0	5.1	1.5
2	71.3	21.5	2.5	3.6	1.1
3	71.9	21.7	1.8	3.6	1.0
4	68.5	20.7	5.4	4.2	1.2
5	64.4	19.5	8.8	5.9	1.4
Total	70.2	21.2	3.6	3.9	1.1

Step 2. Convert SM's absolute differences from baseline to percentage deviations

SM estimate absolute differences from the baseline probabilities in response to changes in temperature. Because the baseline in this analysis differs from theirs in each AEZ, SM's absolute changes are converted to percentage deviations (Table A-13). These percentages are then multiplied by the baseline probabilities in each AEZ to generate the changes in animal choice probability resulting from changes in temperature.

Table A-13 Deviations from Baseline Probabilities in Response to Changes in Climate (%)

	Beef cattle	Dairy cattle	Goats	Sheep	Chickens
Increase temp 2.5C	-14.4	+3.4	+6.8	+28.0	-23.7
Increase temp 5C	-32.2	+17.8	0.0	+73.7	-59.3

Step 3. Develop adjustment factors to scale between calculated results and SM's findings

Using the methods that SM outline for developing the expected income per farm, this analysis attempted to reproduce SM expected incomes based on the original SM selection probabilities, income per animal, and number of animals per farm (i.e., the sum product of these across livestock types). These calculated values are in the third column of Table A-14, and differ from SM's results presented above (and again in the second column of Table A-14). To ensure that the results of this analysis are scaled appropriately to SM's, an adjustment factor is applied to the expected income and each of the changes in expected income. This adjustment factor (fourth column of Table A-14) is applied to each of the country-specific calculations at the AEZ level.

[2] An alternative adjustment approach considered was to divide the total number of each animal type in Ethiopia by SM's estimated baseline livestock per farm Table A-13. This generates the number of farms by primary livestock type, which could be used to generate a distribution of farms by livestock type and substitute for Table A-12. This approach, however, assumes that farms only have one type of livestock, and therefore may significantly overweigh animals that are often kept as a non-primary livestock type.

Table A-14 Adjustment Factors for Differences in Reported and Calculated SM Results

	Predicted Change in Expected Income (US$/farm)		Adjustment Factor
	Reported by SM	Calculated from SM Methods and Results	
Expected income	3,023	2,119	1.43
Increase temp 2.5C	-964	-494	1.95
Increase temp 5C	-2,083	-857	2.43

Step 4. Estimate predicted changes in livestock income in response to incremental changes in temperature

Next, the changes in expected livestock income in each Ethiopia AEZ are generated corresponding to 1°C increases in temperature. First, the baseline expected incomes in each AEZ are estimated, which follows the SM approach outlined above, except that the values are multiplied by the expected income adjustment factor:

Equation 21

$$M^{AEZ} = c^M \sum_l p_l^{AEZ} m_l n_l$$

Where:
M^{AEZ} = Expected income in each AEZ
c^M = Constant adjustment factor to SM results for baseline income
p_l^{AEZ} = Probability of choosing each livestock type in each AEZ
m_l = Income per animal
n_l = Number of each livestock type per farm

These baseline expected income levels are then used to generate changes in expected income under the two temperature increases analyzed by SM based on changes in probability of livestock choice, expected income per animal, and number of animals. Changes for each AEZ and temperature change are shown in the equation below. Note that the second term is the baseline expected incomes prior to adjustment, and that the change relative to that baseline is then multiplied by the appropriate multiplier.

Equation 22

$$\Delta M^{cAEZ} = c^c \sum_l [p_l^{AEZ}(1+\delta_l^{cp})(m_l+\delta_l^{cm})(n_l+\delta_l^{cn}) - p_l^{AEZ} m_l n_l]$$

Where:
ΔM^{cAEZ} = Change in expected income in each AEZ and level of increased temperature c
c^c = Constant adjustment factor to SM results for each of the two levels of increases in temperature c (i.e., +2.5°C, +5°C)
δ_l^{cp} = Percentage change in the probability of choosing each livestock type given a change in temperature c
δ_l^{cm} = Change in income per animal given a change in temperature c
δ_l^{cn} = Change in number of each livestock type per farm given a change in temperature c

Table A-15 provides the results of this procedure both in terms of the mean expected change in income and the percent change from baseline levels. The key numbers in the table are shaded in gray; these are percent changes in expected income resulting from incremental changes in climate, and would be applied directly to the development of the response of livestock to climate between

2001 and 2050. As described below, because the percentage changes in Table A-15 exceed the reported percentage changes of SM, the SM values are adopted for the climate change assessment.

There are three important observations of note on Table A-15:

- The expected incomes are nearly triple those estimated by SM. This is because of the much higher probability of choosing more profitable beef cattle over goats, sheep, and chickens in Ethiopia as compared to SM's average case for Africa.[3]
- The deviations in response to climate vary minimally across AEZs. This is because beef cattle and chickens are the primary drivers of changes in expected income, and neither chickens nor beef cattle probabilities vary significantly across AEZs. As a result, expected incomes (presented below) respond primarily to differences in AEZ climate rather than livestock distribution.
- Temperature increases to 5°C result in losses that exceed those estimated by SM (i.e., 32 percent and 69 percent resulting from a 2.5°C and 5°C increase in mean temperatures). Losses are capped in the analysis of climate effects (described below) at these SM estimates to avoid generating estimates outside of their predicted ranges. These translate to a 12.8 percent reduction in expected incomes per degree of temperature increase from zero to 2.5°C, and a 14.8 percent reduction per degree from 2.5°C to 5°C respectively. These estimates, rather than those in Table A-15, are utilized in developing the vectors of projected livestock effects.

Table A-15. Mean Expected Changes in Income Resulting from Changes in Temperature, and Percent Changes from Baseline

	Mean (US$/farm)					Percent Change from Baseline				
	AEZ 1	AEZ 2	AEZ 3	AEZ 4	AEZ 5	AEZ 1	AEZ 2	AEZ 3	AEZ 4	AEZ 5
Expected Income (Base)	9,377	10,397	10,483	9,999	9,428					
Increase temp 2.5°C	-4,598	-5,108	-5,151	-4,909	-4,621	-49.0	-49.1	-49.1	-49.1	-49.0
Increase temp 5°C	-9,609	-10,682	-10,772	-10,263	-9,656	-102	-103	-103	-103	-102
Per 1° change to 2.5°C	-1,839	-2,043	-2,060	-1,964	-1,849	**-19.6**	**-19.7**	**-19.7**	**-19.6**	**-19.6**
Per 1° change 2.5 to 5°C	-2,004	-2,230	-2,248	-2,142	-2,014	**-21.4**	**-21.4**	**-21.4**	**-21.4**	**-21.4**

Step 5. Evaluate the Effects of Climate

Next, the incremental effects of changes in temperature (i.e., 12.8 to 14.8 percent reductions per degree of increased temperature) are applied to the base case scenario and the four climate change scenarios in each AEZ to generate vectors of changes in expected farm incomes from baseline conditions. Because these are expected values, they are interpreted broadly to represent changes in livestock incomes across Ethiopia. In total, five of these vectors are generated for each AEZ, or 25 in total. Here, "baseline conditions" are defined as the mean temperature in the base case scenario; as such, all results presented here are deviations from that baseline. Note that changes in temperature from the baseline mean sometimes exceed 5°C; in these cases, temperature changes are capped at 5°C in order to remain within the bounds of SM's range of analyzed scenarios.

[3] In the Ghana livestock analysis, where chickens are the dominant TLU, this approach produced expected incomes as low as $1,500 per farm.

Annex 8
Drought Model Details

Data on Dependent Variable

Available data on government expenditures on VFS are presented in Table A-16. These represent one spending category within Ethiopia's Agricultural and Rural Development (ARD) fiscal database (World Bank 2008). Total annual expenditures range from $127 million in 1997/98 to $3.6 billion in 2004/05 (in 2010 U.S. dollars), and are composed of recurrent and capital expenses. This analysis uses recurrent VFS expenditures—which are more likely to capture the food- and labor-related costs of responding to drought—as the dependent variable in the reduced form model that will project drought expenditures under the five scenarios. Of the total expenditures, recurrent costs range from $34 million in 2005/06 to $1.8 billion in 2003/04. As noted above, the sharp increase in spending starting in 2001/02 was due to a special purpose grant for food security. We address this issue statistically as explained below.

Table A-16. Ethiopian Government Expenditures on Vulnerability and Food Security (Millions of 2010 US dollars)

Expenditure Category	1997/ 98	1998/ 99	1999/ 00	2000/ 01	2001/ 02	2002/ 03	2003/ 04	2004/ 05	2005/ 06
Vulnerability and Food Security	**127**	**134**	**309**	**270**	**2,088**	**1,083**	**3,329**	**3,564**	**2,517**
Recurrent	119	121	298	224	1,626	596	1,829	1,417	34
Capital	8	13	10	45	463	488	1,501	2,147	2,483

Source: World Bank (2008).

It is important to note that the dependent variable in this analysis is limited in both its temporal and spatial resolution (that is, only nine years of annual data for all of Ethiopia). Although finer resolution data would produce more statistically robust results, these nine years of expenditures occurred over a period of highly variable climate, and therefore may provide a reasonable characterization of the relationship between changing future climate and government expenditures on VFS.

Data on Independent Variables

Drought indicator data. First, data on possible climatic drivers of VFS expenditures were gathered. Because drought is most damaging when it occurs over multiple consecutive months, this analysis would ideally rely on a drought index that combines temperature and precipitation data at the seasonal temporal scale to capture the important duration dimension of drought. Although several indices in the U.S. have been used to capture duration of droughts, such as the Palmer Drought Severity Index (PDSI; see Palmer 1965) or the Standardized Precipitation Index (SPI; see McKee et al. 1993), development of these indices for Ethiopia was not feasible given the scope of this analysis.

Instead, the analysis considers (a) annual crop yields (desirable because they partly integrate climate conditions over multi-month periods), (b) mean monthly precipitation, (c) mean daily temperature, and (d) mean maximum daily temperature. These are shown for 1997 to 2006 in Table A-17, although only 1998 to 2006 data were employed in the statistical model because the majority of each Ethiopian calendar year falls on the second Gregorian year (e.g., January 1 to September 10 of 1998 fall in 1997/98). To generate the percentage of maximum crop yield estimates, outputs of CLICROP, a crop process model, were used for seven key Ethiopian crops (barley and other grains, maize, millet, sorghum, soybeans, spring wheat, and teff). Crop yields were combined in a weighted average based on the spatial coverage of each crop. The NASA POWER daily dataset was the source of the remaining data. Both CLICROP and NASA data were at 1° by 1° resolution over Ethiopia; these were spatially averaged over the region affected by droughts (described below) between 1997 and 2006. Note that the variation in annual precipitation is much more pronounced than variations in annual yields or temperatures.

Table A-17. Climate Variables within Areas Experiencing Drought between 1997 and 2006

Year	Percentage of Maximum Crop Yield	Mean Monthly Precip (mm)	Max Temp (°C)	Mean Temp (°C)
1997	66.8%	58.8	28.9	24.1
1998	67.3%	51.9	29.7	24.9
1999	64.3%	54.6	28.9	24.0
2000	61.0%	38.3	29.7	24.3
2001	67.9%	45.8	29.1	23.8
2002	63.2%	47.2	29.5	24.2
2003	64.7%	45.3	29.4	24.1
2004	64.8%	45.1	28.7	23.8
2005	71.1%	52.0	28.6	24.0
2006	67.8%	61.0	28.2	23.8

In order to consider those regions where expenditures on VFS were most likely being directed, the analysis focuses on the geographic areas that have experienced significant droughts over the period between 1997/98 and 2005/06. For this information, the analysis relied on the World Bank EACC Ethiopia Case Study document entitled "Learning from Past Experiences with Extreme Climate Events" (Zeleke et al. 2010). The following droughts were recorded during the period of interest:

- **1999/00 drought.** Affected 4.9 million people in the North Wello and East Hararge zones in the South Oromiya region.
- **2003/04 drought.** Affected 13.2 million people in the Tigray, Oromiya, Amhara, Somali, and Afar regions.
- **2005/06 drought.** Affected 2.6 million people in the Afder, Liben, and Gode zones in the Somali region, and the Borena zone in the Oromiya region.

Given the size of the Oromiya and Somali regions (affected during the 2003/04 drought), the analysis focuses on the Liben, Afder, and Gode zones within the Somali region, and the Borena zone in Oromiya, each of which was also affected during the 2005/06 drought. The regions and zones of Ethiopia are presented in Figure A-16.

Figure A-16. Map of Regions and Zones within Ethiopia

***Source*: UNDP Emergencies Unit for Ethiopia (2000). Map provided by ReliefWeb at http://www.reliefweb.int.**

Dummy Variable to Account for Federal Special Purpose Grant

The significant increase in drought expenditures in 2001/02 resulted from a federal special purpose grant for food security. As noted by the World Bank (2008), several external funding sources (e.g., World Bank, EU direct budget support program for food security) were responsible for a portion of this grant and thus some fraction of the spending was not sourced from Ethiopian government funds. Because this fraction is unknown, this analysis uses an average of the dummy value over the nine-year period (0.556) in making projections from the statistical formulation.

Model Formulation

Several possible models were tested to evaluate which best explained variation in VFS expenditures. Overall, the temperature and yield variables fit very poorly, but precipitation fit well, as did the grant dummy variable. Interestingly, data on percentage of Ethiopian population affected by drought from Zeleke et al. (2010) had no relationship to VFS expenditures.

The final model, which involved the natural log of the VFS expenditures (due to the high degree of variation between values), was as follows:

Equation 23

$$\ln E^{VFS} = \beta_0 + \beta_1 P + \beta_2 G$$

Where:
E^{VFS} = Expenditures on VFS
P = Precipitation
G = Dummy indicating presence of the special purpose grant for food security (0 from 1997/98 to 2000/01 and 1 from 2001/02 to 2005/06)

The model had a multiple R^2 value of 0.82 and both of the explanatory variables were significant at the 5 percent level; summary statistics for the intercept and independent variables are summarized below in Table A-18.

Table A-18. **Summary Statistics**

	Coefficient	Standard Error	t Stat	P-value
Intercept	11.925	2.429	4.910	0.003
Precipitation	-0.142	0.050	-2.832	0.030
Grant dummy	1.595	0.630	2.531	0.045

Because of the small sample size, the reduced form model was tested for robustness and influential observations by running nine models with one observation removed from each. In these nine regressions, the intercept coefficient ranged from 7.3 to 14.5, the precipitation coefficient ranged from -0.19 to -0.045, and the coefficient on the grant dummy variable ranged from 1.30 to 1.96. The relatively tight ranges of these coefficient estimates indicate that the model is not being influenced heavily by individual observations.

Prediction of Drought Expenditures

Next, 2001–50 precipitation projections were incorporated into the above statistical relationship to predict drought expenditures under the baseline and four climate scenarios. In the absence of information on the balance of internal and external funding resources in future years, the analysis uses the mean of the grant dummy value (0.556) in the prediction equation.

The prediction equation for drought expenditures is:

Equation 24

$$E^D = e^{11.925-0.142P+1.595*0.556}$$
$$= e^{12.81-0.142P}$$

Where:
E^{VFS} = Expenditures on VFS
P = Precipitation
G = Dummy indicating presence of the special purpose grant for food security

Figure A-17 shows the precipitation projections under the baseline and four climate scenarios in regions and zones of Ethiopia that experienced drought between 1997 and 2006. Note that average monthly precipitation each year varies widely, from just over 30mm in 2034 in the Ethiopia dry scenario to over 135 mm in 2011 in the global wet scenario. These differences generate large variations in drought expenditures in the reduced form model.

Figure A-17. **Mean Monthly Precipitation in Regions of Ethiopia Experiencing Severe Drought, 1997–2006**

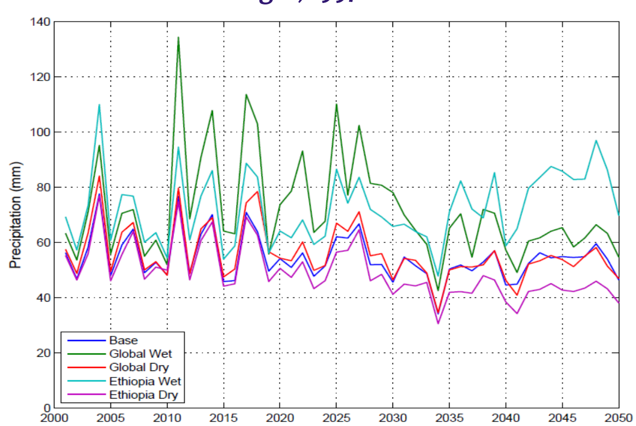

Key Assumptions

This screening-level modeling effort develops statistical correlations between VFS expenditures and the explanatory variables described above to project future expenditures. In the absence of additional information on this relationship, this analysis is unable to identify causal relationships between expenditures and these explanatory variables. This analysis of drought expenditures has several key assumptions:

- Expenditures on VFS are entirely attributable to droughts. The World Bank has indicated that a sizeable percentage of VFS expenditures (including the increase in 2001/02) have been directed at programs that have no connection to drought response.[4] As a result, this analysis likely overestimates the cost of droughts. Provided more specific information on the fraction of VFS expenditures that are on droughts, this analysis would generate more precise estimates.
- Expenditures on VFS wholly account for government expenditures on droughts. The World Bank has noted that a large fraction of drought response is through food aid rather than dollars, which is not captured in the expenditures data.[5] Were the costs of this food aid included in VFS expenditures, this analysis would likely estimate higher drought-related costs.
- Only recurrent expenditures, not capital expenditures, are caused by drought. Given that a certain but unknown fraction of capital expenditures are related to drought response, this assumption likely understates the cost of droughts.
- Historical patterns of expenditures on VFS are representative of spending patterns in future years. Whether this assumption holds is uncertain.

The expenditures on VFS as presented by the World Bank (2008) were primarily from the Ethiopian government rather than from international donors. The World Bank acknowledges that a certain fraction is from international donors, but that larger internationally funded efforts were not included in their expenditure figures. The grant dummy variable partly accounts for this effect.

[4] Specifically, many of the expenditures unrelated to the special purposes grant are for chronically food-insecure households rather than for those that experience drought-related food shortages. Much of the special purpose grant funds were directed at rural infrastructure, livelihood diversification, and resettlement. Based on written correspondence with Laketch Mikael, Senior Rural Development Specialist, World Bank AFTAR/Ethiopia, on September 8, 2010.

[5] Based on written correspondence with Laketch Mikael, Senior Rural Development Specialist, World Bank AFTAR/Ethiopia, on September 8, 2010.